Journal of Power Sources 185 (2008) 867–870

Contents lists available at ScienceDirect

Journal of Power Sources

journal homepage: www.elsevier.com/locate/jpowsour

Short communication

# X-ray imaging of water distribution in a polymer electrolyte fuel cell

Sang Joon Lee [a,*], Nam-Yun Lim [a], Seok Kim [a], Gu-Gon Park [b], Chang-Soo Kim [b]

[a] *Department of Mechanical Engineering, Pohang University of Science and Technology, San 31, Hyoja Dong, Namgu, Pohang 790-784, Republic of Korea*
[b] *PEFC Research Group, Korea Institute of Energy Research, 71-2 Jang-dong, Yuseong-gu, Daejeon 305-343, Republic of Korea*

ARTICLE INFO

*Article history:*
Received 19 May 2008
Received in revised form 22 July 2008
Accepted 29 August 2008
Available online 18 September 2008

*Keywords:*
Polymer electrolyte fuel cell
Water management
X-ray imaging
Digital image processing

ABSTRACT

At present, water management in a polymer electrolyte fuel cell (PEFC) is a major subject of research. In fact, proper water management is vital to achieve maximum performance and durability from a PEFC. Consequently, this study is conducted to visualize quantitatively the water distribution in a PEFC by means of an X-ray imaging technique. The X-ray images of the PEFC components with and without water are clearly distinguished. Reference to the visualized X-ray images, enables quantitative evaluation of the water distribution in the region between the separator and the gas-diffusion layer (GDL). Likewise, the meniscus of water in the channels of the PEFC is clearly observed.



## 1. Introduction

The polymer electrolyte fuel cell (PEFC) provides clean and highly efficient energy and has been extensively studied as a power source for electric vehicles. The PEFC is composed of an electrolyte membrane, an electrode catalyst, a gas-diffusion layer (GDL), bipolar plates, etc. Nafion is usually employed as the electrolyte membrane; it has proton conductivity only in the presence of water. Therefore, gases supplied to the fuel and to the air electrodes should be humidified for efficient transportation of the protons. While much moisture is beneficial for the electrolyte membrane, excessive moisture can deteriorate the performance of the fuel cell. It can specifically affect the electrode catalyst, the GDL, and the bipolar plates. Thus, proper water management, including efficient supply and drainage of water, is definitely important for the efficient operation of the fuel cell [1]. As such, water management in PEFC is one of inevitable issues in the commercialization process of PEFC [2].

Various research investigation of water management have been performed recently. Most of these have focused on the visualization of the water distribution inside the PEFC. For example, Geiger et al. [3] observed the water distribution inside a functioning PEFC using a neutron image technique. In addition, water distribution in a PEFC was visualized through magnetic resonance imaging (MRI) [4] and by an X-ray tomography technique [5]. Likewise, the flow and distribution of water inside a PEFC was investigated using a transparent unit cell [6].

Meanwhile, Myers [7] reported that the amount and the distribution of water existing inside a PEFC could play an important role in its durability. Yang et al. [8] studied the generation, removal and regeneration of water drops in the channels of a transparent unit cell with the progress of operation time. They confirmed that the water drops contacted closely to the surface of the channels. In spite of this, they were not able to measure the exact quantity of water that had been produced and accumulated inside the fuel cell. Similarly, Owejan et al. [9] investigated the quantity and distribution of water in a PEFC using a neutron imaging technique. The findings were limited, however, due to a technical constraint in the selection of the cell materials.

The neutron image technique for examining water distribution is more expensive and has a lower spatial resolution, than the X-ray image technique. With MRI, visualization of water inside the GDL is difficult because of the magnetically inductive materials, such as carbon, that are used in the fuel cell. Sinha et al. [5] measured the distribution of water inside the GDL of a PEFC by means of the X-ray micro-tomography with the lapse of purging time. The measurement technique was limited to the GDL and the characteristics of the materials of the flow channel, which affect the drainage of water, could not be investigated.

The X-ray image technique has been used in the work reported has because, given the temporal and spatial resolution, it has strong potential for the visualization of water inside a PEFC.

Images are obtained of the water at the GDL and the separator, which has micro-channels and is made of carbon. Also, the feasi-

* Corresponding author. Tel.: +82 54 279 2169; fax: +82 54 279 3199.
*E-mail address:* sjlee@postech.ac.kr (S.J. Lee).

0378-7753/$ – see front matter © 2008 Elsevier B.V. All rights reserved.
doi:10.1016/j.jpowsour.2008.08.101

bility of quantitative measurement of water contents in the PEFC is examined.

## 2. Experiment

In a conventional X-ray tube, the high voltage induces an electric field between the anode and the cathode. The accelerated electrons in the electric field collide with the anode and X-rays are generated by the energy transformation in the collision. The energy of an accelerated electron can be expressed as a multiplication of the electric charge and the external voltage, i.e., $E = \mathrm{eV}$. More than 99% of the transformed energy in the electronic collision becomes heat and then dissipates.

In order to resolve the heating effect of kinetic energy, the anode is commonly capable of rotating for efficient cooling and is usually made of tungsten or molybdenum, both of which can tolerate high temperatures. The X-ray is generated by transformation of small part of the kinetic energy of accelerated electrons and propagates in a cone shape. The intensity of X-rays passing through a test sample can be expressed by:

$$I = I_o\, \mathrm{e}^{-\mu x} \tag{1}$$

where $I$ is the intensity of the X-ray attenuated after penetrating the test sample; $I_o$ represents the initial intensity of the incident X-ray; $\mu$ is the attenuation coefficient for the sample. The attenuation coefficient $\mu$ generally increases as the density or atomic number (Z) increases. The mass attenuation coefficient ($\mu/\rho$) can be obtained by dividing $\mu$ by the density ($\rho$). A material has its own inherent mass attenuation coefficient for a specific radioactive ray. When the test sample is composed of several constituents having different refractive materials, absorption contrast in the X-ray images can be obtained.

In order to obtain clear X-ray images, a compact imaging system has been developed using a medical X-ray tube that served as a light source. The X-ray tube (Varian A272) has a small focal spot size of 0.3/0.6 mm at 200/500 mA for 40∼160 kvp. The pixel size of the conventional X-ray detectors used in clinical radiography is usually larger than 50 μm. However, in this study, a customized X-ray CCD camera that has a spatial resolution of 4000 × 2672 pixels is used. The pixel size of the CCD camera is 9 μm and a cesium iodide (CsI) scintillation crystal is fixed to the top surface of the CCD sensor array. Due to the high sensitivity of the CsI scintillator, the CCD camera can be used to acquire X-ray images directly, with any gold-coated mirror. The X-ray CCD and tube were synchronized via an external trigger switch by using a photocoupler chip and a transistor-transistor logic (TTL) signal from a delay generator. A photograph of the X-ray imaging system is given in Fig. 1.

The PEFC components tested in this study are separators made of graphite and the GDL (10BC, SGL Inc.). The separator has gas channels of 1.2 mm in width and 0.8 mm in depth. In addition, acyl is used as the end-plate because a material with high atomic number, such as gold, has a large attenuation coefficient for an X-ray beam.

## 3. Results and discussion

### 3.1. Digital image processing

The X-ray beam generated from the X-ray source has a slight deviation in terms of light intensity with time. Since it passes through the scintillator that is installed in front of the CCD camera, the light intensity at each pixel is slightly different due to time. In this study, a digital image processing technique was adopted to reduce the occurrence of unwanted noise, and to quantify the light intensity between the water and the separator rib. In the digital image processing, reduction of noise is essential before the quantitative analysis of water distribution is performed. In order to achieve this, a non-linear digital filtering technique, often with the use of a median filter, is applied to remove the noise embedded in the optical images. A median filter is used in examining a sample of the input data; thereafter it has to be decided whether or not it is a representative of the signal. Such a procedure has been adopted using a window that consists an odd number of samples. Moreover, the values in the window are sorted in numerical order. The median value, i.e., the sample in the centre of the window, is selected as the output. After discarding the oldest sample, a new sample is acquired, and the calculation process is then repeated. The median

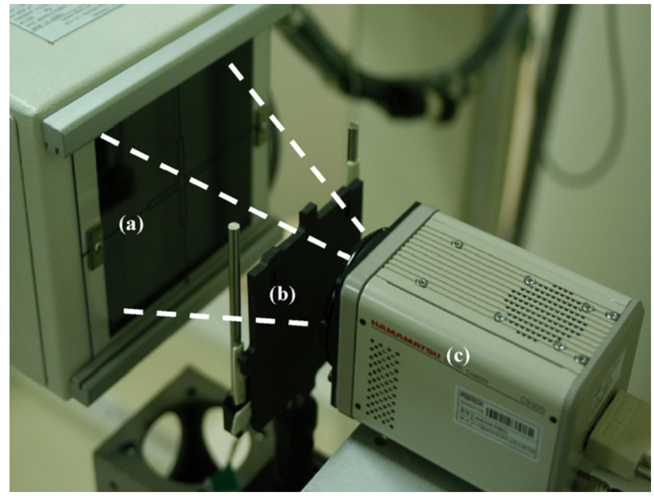


**Fig. 1.** X-ray imaging system for fuel cell experiments: (a) X-ray tube, (b) fuel cell components, and (c) X-ray CCD camera.

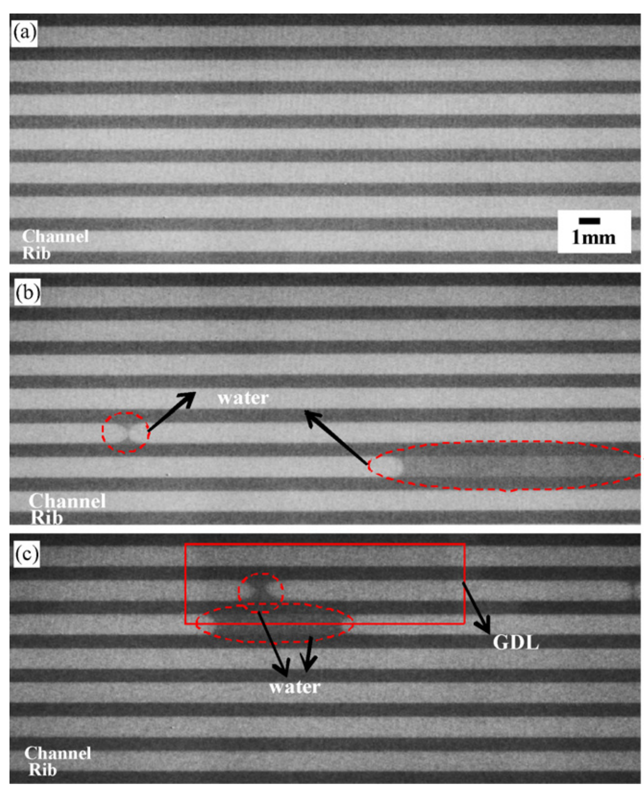


**Fig. 2.** X-ray images of (a) separator only, (b) separator and water, and (c) acryl plate, separator, water and GDL.

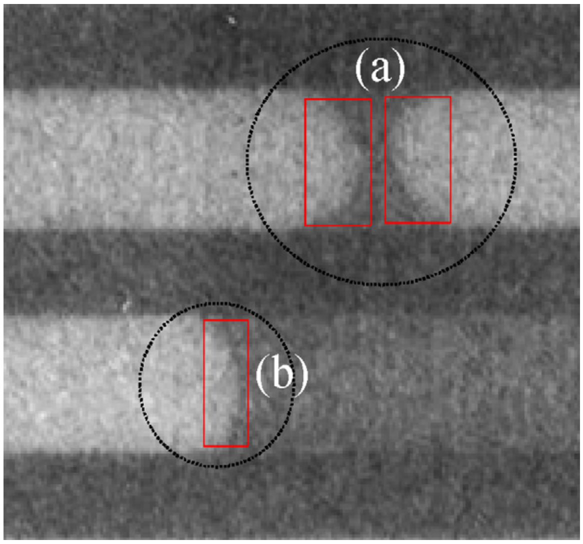


**Fig. 3.** Configuration of meniscus between water and air in channel of separator: (a) with GDL and (b) without GDL.

filter does not create new unrealistic pixel values when the filter straddles at the edge because the median value has to be the value of one of the pixels in the group. For this reason, the median filter is better used for preserving sharp edges, compared with the other filters.

### 3.2. *X-ray imaging of water distribution*

A typical X-ray image of the separator with micro-channels is shown in Fig. 2(a). In this image, the gas channels appear in grey and the ribs in black. The contrast in X-ray images is formed due to

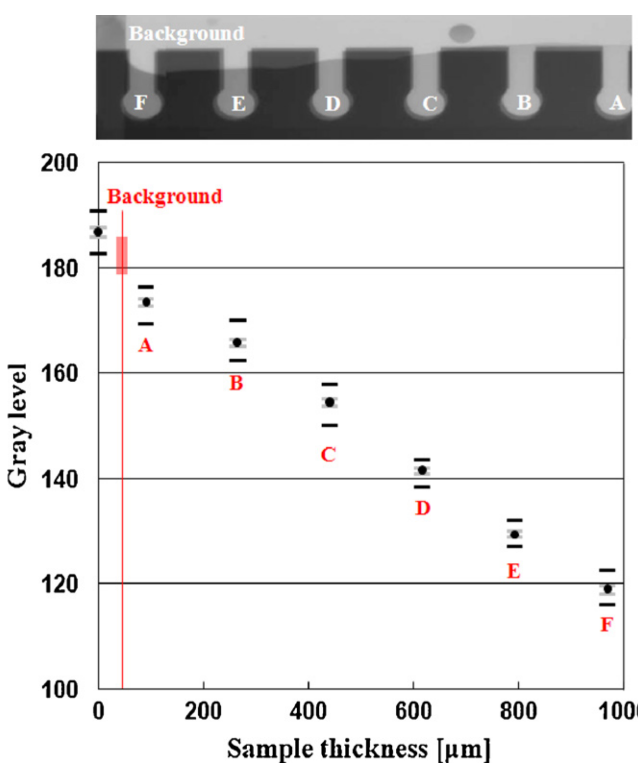


**Fig. 4.** Variation of grey level according to sample thickness (a) $t = 0.09$, (b) $t = 0.27$, (c) $t = 0.44$, (d) $t = 0.62$, (e) $t = 0.79$, and (f) $t = 0.97$ mm.

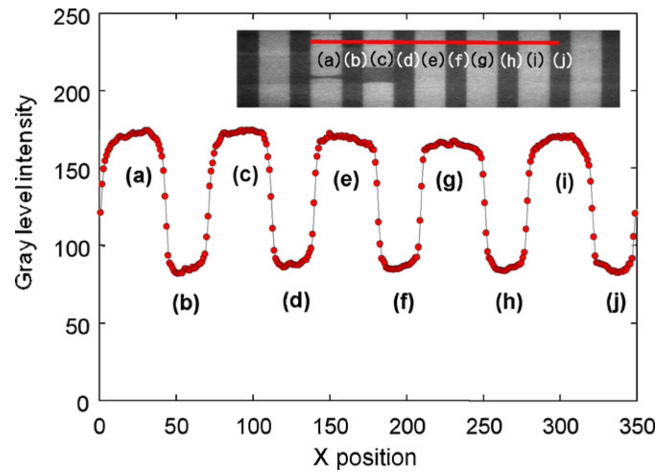


**Fig. 5.** Grey level profile across channels and ribs of separator.

the difference in X-ray absorption rates between the materials from which the test sample is composed. The attenuation coefficient of a material increases with its atomic number. As the ribs of the separator are thicker than the channels, they have a relatively large attenuation coefficient and thereby give use to more brightness in the absorption of the contrast image.

To check the existence of water in the separator, a small amount of water was dropped on its channels. The resulting X-ray image is shown in Fig. 2(b). The water can be clearly distinguished from other materials. In addition, it is possible to observe the meniscus of water and its contact angle in the micro-channels of the separator.

The captured X-ray image of the water distribution when the three main components of a PEFC, namely, acrylic plate, separator and GDL are assembled. Water was dropped on the channels of the separator, and then the GDL and acrylic plate were attached. The acrylic plate of 25 mm thickness, separator, water and GDL were arranged in sequence from the direction of the X-ray tube. The attenuation coefficient of the acrylic plate appeared to be sufficiently low. Thus, there is no difficulty in distinguishing one component from the others in the X-ray image, although the image was a little darker than those shown in Fig. 2(a) and (b).

The meniscus between water and air in the channel of the separator with and without the GDL is clearly visible in Fig. 3. The meniscus of the water in the presence of GDL has a larger curvature than that of the water in the absence of GDL. This is probably due to

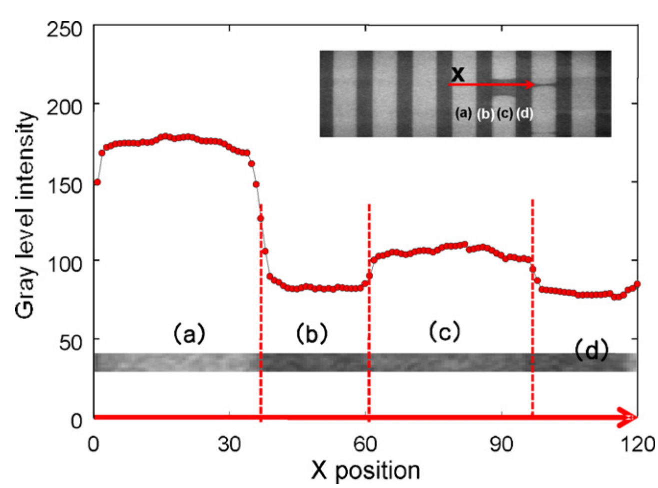


**Fig. 6.** Variation of grey level along a horizontal line passing through liquid layer.

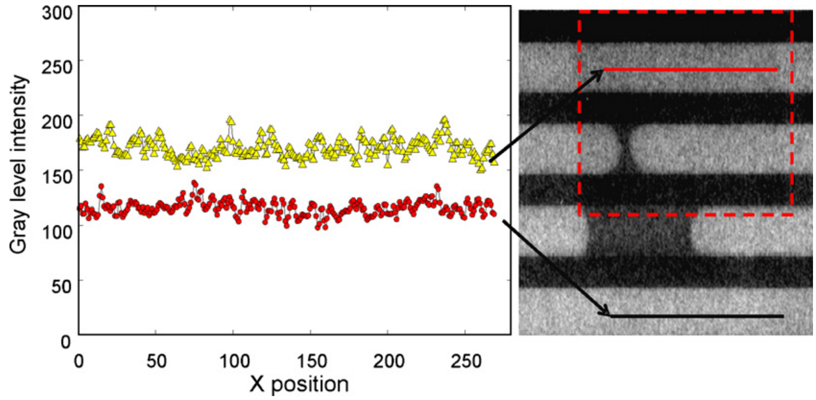


**Fig. 7.** Effect of GDL on variation of grey level along horizontal line.

the hydrophobicity of the polytetrafluoroethylene (PTFE) contained in the GDL.

### 3.3. *Water distribution and quantification*

A calibration device with six sample holders of different depth was made to check the feasibility of quantifying the water by using the grey level of the X-ray images. After filling up the sample holder with iopamidol (used as an X-ray contrast medium), X-ray images were obtained and the grey levels extracted. The results are presented in Fig. 4. The grey level decreases linearly with increase in the thickness of the sample. The grey level of the thickest sample ($t$ = 0.97 mm in thickness) is 120, while that of the thinnest sample ($t$ = 0.09 mm) is 175. This indicates that 17 μm difference in water thickness may change one digit in the value of grey level. Based on these results, we can see that the variation of in grey level according to water thickness will enable the quantification of water distributed inside the PEFC.

The grey level profile along an arbitrary horizontal line across the channels and ribs of the separator is presented in Fig. 5. The channel part of the separator shows a large value of the grey level (170), while the rib reports a low value (70). This indicates that the rib part has a large attenuation coefficient.

The variation in grey level along a horizontal line, which cuts across the channel-containing water is given in Fig. 6. Sections (a)–(c) represent the channel without water, the rib, and the water-containing channel, respectively. The difference in grey level between sections (a) and (c) is about 70 and this clearly confirms the presence of water in the channel or in the rib of the separator.

The effect of the GDL on the grey level difference is shown in Fig. 7. The dashed box on the X-ray image represents the piece of GDL laid over the separator. As shown in Fig. 4, the grey level is decreased by 50 in the presence of the GDL, compared with that in the absence of the GDL.

## 4. Conclusions

The X-ray CCD camera has a high spatial resolution of 9 μm. Thus, the presence of water inside the several components of a PEFC is visualized quantitatively by using the X-ray imaging technique. Similarly, the meniscus of the water in the channels of the separator is clearly observed. In addition, to remove unwanted noise for quantitative analysis, a digital image processing technique has been adopted. The grey level of water in the X-ray image decreases linearly as the water thickness is increased. Therefore, the water distribution between the separator and the GDL is quantitatively determined, and the feasibility of the method for determining water distribution inside PEFCs is conformed.

## Acknowledgements

This work was supported by the Korea Science and Engineering Foundation (KOSEF) through the National Research Laboratory Program funded by the Ministry of Science and Technology (M10600000276-06J0000-27610) and by the Korea Institute of Energy Research.

## References

[1] K.W. Feindel, S.H. Bergens, R.E. Wasylishen, Chem. Phys. Chem. 7 (2006) 67–75.
[2] M.M. Mench, Q.L. Dong, C.Y. Wang, J. Power Sources 124 (2003) 90–98.
[3] A.B. Geiger, A. Tsukada, E. Lehmann, P. Vontobel, A. Wokaun, G.G. Sherer, Fuel Cells 2 (2003) 92–98.
[4] Z. Dunbar, R.I. Masel, J. Power Sources 171 (2007) 678–687.
[5] P.K. Sinha, P. Halleck, C.Y. Wang, Electrochem. Solid-State Lett. 9 (7) (2006) A344–A348.
[6] F.Y. Xhang, X.G. Yang, C.Y. Wang, J. Electrochem. Soc. 153 (2) (2006) A225–A232.
[7] J.P. Meyers, Fundamental issues in subzero PEMFC startup and operation, in: Workshop on Fuel Cell Operations at Sub-freezing Temperatures, Washington DC, February 1–2, 2005.
[8] X.G. Yang, F.Y. Zhang, A.L. Fubawy, C.Y. Wang, Electrochem. Solid-State Lett. 7 (11) (2004) A408–A411.
[9] J.P. Owejan, T.A. Trabold, D.L. Jacobson, D.R. Baker, D.S. Hussey, M. Arif, Int. J. Heat Mass Transfer 49 (2006) 4721–4731.